AFFDL TM 72-22 FX

AIR FORCE FLIGHT DYNAMICS LABORATORY
DIRECTOR OF LABORATORIES
AIR FORCE SYSTEMS COMMAND
WRIGHT PATTERSON AIR FORCE BASE OHIO

TOTAL ENTHALPY MEASUREMENT FROM BLUNT BODY GAS CAP EMISSION IN ARC-HEATED WIND TUNNELS: RESULTS AND APPLICATION

By

L. R. Lawrence, Jr.
R. E. Walterick
T. M. Weeks
J. P. Doyle, Jr.

20000501 085

25 July 1972

Reproduced From
Best Available Copy

Flight Mechanics Division
Air Force Flight Dynamics Laboratory
Wright-Patterson AFB, Ohio 45433

Approved for Public Release: Distribution Unlimited

FOREWORD

This report was prepared by L. R. Lawrence, Jr., Ronald E. Walterick, and Thomas M. Weeks of the Analysis Group and by Joseph P. Doyle, Jr., chief of the Thermomechanics Branch, Flight Mechanics Division, Air Force Flight Dynamics Laboratory, Wright-Patterson Air Force Base, Ohio. The work was performed in house in support of ABRES project no. 627A and covers work conducted between September 1970 and May 1971.

This technical memorandum has been reviewed and is approved.

Philip P Antonatos

PHILIP P. ANTONATOS
Director
Flight Mechanics Division
AF Flight Dynamics Laboratory

AFLC—WPAFB—AUG 72 30

Symbols

A_n^m - Einstein coefficient for a transition from electronic state m to state n.

E - Energy

g - Statistical weight

h - Planck's Constant

I - Intensity

k - Boltzmann Constant

N - Species number density

p - pressure

T - Temperature

U - velocity behind the shock in the x-direction

x - axial distnace through the shock layer measured from the front of the shock wave.

Z_o - Partition function

γ - Specific heat ratio

δ - collision loss factor

ν_c - collision frequency

ν_o - spectral frequency of a copper line

τ - Nitrogen vibrational relaxation time constant.

Subscripts and Superscripts

c - collisional

e - pertaining to free electrons

i - initial value immediately behind the shock front

m - upper state

n - lower state

o - total or stagnation value

r - pertaining to rotational modes

s - static property behind the shock front

t - pertaining to translational motion

v - pertaining to vibrational modes

1 - condition just before the shock front

Introduction

At the Air Force Flight Dynamics Laboratory, there has been a continuing program to measure total enthalpy during test conditions in which heating rates are above 5000 BTU/ft^2-sec. Below this level of heating, steady state enthalpy probes and steady state calorimeters can be successfully employed to determine total enthalpy[1]. However, above 5000 BTU/ft^2-sec, in an important region for re-entry testing, the heating is so severe that only transient probes can be employed[2,3]. When using transient probes (calorimeters or enthalpy probes), empirical corrections must be made, and Fay and Riddell's theory[4] must be applied in order to determine total enthalpy. This is complicated by the fact that the enthalpy is not uniform for many test conditions, and may vary across the flow by a factor between 2 and 4. Therefore, the transient probes must have response characteristics of high enough quality to measure an enthalpy distribution, rather than just one value of total enthalpy. This is further complicated by heater unsteadiness effects.

A typical result of transient probes is shown in Figure 1 for a "peaked" enthalpy distribution in the

re-entry test section. The maximum of the presented heat flux curve corresponds to the maximum enthalpy, which is approximately at the flow centerline. The heat flux curve was generated by sweeping a calorimeter across a 2.8cm nozzle exit at a constant rate of 76cm/sec, and the results are uncorrected for heater unsteadiness effects.

In June 1971, a conceptual paper[2] was presented at the International Congress on Instrumentation in Aerospace Engineering Facilities. The paper delineated two possible methods of using spectroscopy to circumvent the problems associated with transient probe measurement of total enthalpy. It was suggested that an examination of the radiant emission from stagnation gas caps on blunt bodies under test could result in a measurement of total enthalpy. The two approaches suggested were: a) an examination of the continuum emission, and, b) an analysis of the emission due to electronic transitions in trace amounts of gaseous copper in the flow. The examination of the continuum emission, described in reference 2, has proven fruitless due to optical thinness, heater unsteadiness, and the lack of a well-defined continuum peak. The method of analyzing

the line emission from gaseous copper has proven to be useable and valuable for both on-line testing and heater calibration. For heating conditions above 5000BTU/ft^2-sec, it is now possible to determine average test section total enthalpy during the same time that a model is being tested.

Unsteadiness Effects

The heater unsteadiness properties have been examined theoretically by Weeks[5] and experimentally by Van Kuren[6]. Some of the experimental results of Van Kuren are presented in Figure 2. Copper lines at 5106, 5153, and 5218 Å were examined over a period of time to determine their fluctuation properties. The intensity variation was found to be characteristically at a frequency of 100hz with an amplitude of $\pm$ 12%.

Based on the work of Weeks[5] and Webber and Garscadden[7], significant errors would be incurred if a spectrum was taken over a time period greater than or equal to the period of oscillation of the arc heater. The error would be due, basically, to the fact that intensity and temperature are logarithmically related, such that the average (or integrated) intensity, over

a number of oscillations, would not give the correct average temperature. The temperature (or enthalpy) error introduced by unsteadiness effects would be approximately 5% for a ± 12% intensity variation at a temperature of 5000°K. Small amplitude unsteadiness evidence has been found at 300Khz, but the effects are negligible since the amplitude of the high frequency unsteadiness is only on the order of ± 1%.

Apparatus

The apparatus employed in this work had to be chosen so as to avoid heater unsteadiness problems; therefore, the basic piece of apparatus used to take the necessary data is an OCLI type 501 Rapid-Scanning Spectrometer. This instrument has a sequence of corner mirrors which sweep through an intermediate focal plane of a double pass Czerny-Turner grating spectrometer to produce up to 800 spectral scans per second. For radiance measurements, a reference source is contained in the Model 501 for intensity calibration. As long as the entrance aperture is fully illuminated and the focused image fills the entrance slit, the radiance calibration of the system is independent of focus or

object distance. The instrument is operated in a mode wherein a spectrum from 2500 to 6500 Å is taken with 4 Å resolution in the space of a millisecond. Only a small portion of the spectrum is analyzed for the total enthalpy measurement, such that the time spent in recording this small spectral region is on the order of 50 microseconds. This is well within the 10 millisecond characteristic period of oscillation of the flow field intensity.

The focussing of the optics is accomplished with a Cassegrainian telescope which is an integral part of the spectrometer. The entrance slit is focussed with reverse optics onto the region just in front of the blunt-body to be examined (Figure 3). In this way, a section of the gas cap can be examined which is less than 1 mm in width, and the focussing can be done such that ablation products do not interfere with the portion of spectrum to be examined. This focussing is sufficient since the characteristic gas cap thickness is between 1.5 and 5.5 mm.

The data is taken by displaying the output of the spectrometer on a Tektronix type 555 oscilloscope and expanding the horizontal display such that only the

desired portion of the spectrum is presented. A 35 mm framing camera is used to record the oscilloscope traces at 40 frames per second, and 2 msec per frame. In this way, only one spectral datum is recorded on each frame. The resulting portions of film are enlarged to 8x10 prints which are then analyzed by a method described in a later portion of the paper.

Theory

In examining the various portions of the spectrum which could be used for flow property analysis, it is found that the most prominent characteristics are several spectral lines, resulting from electronic transitions in atoms of gaseous copper. The more prominent of these lines are at 3248, 3274, 5106, 5153, 5218, 5700, and 5782 Å. In order to use any of these lines for diagnostic purposes, several assumptions have to be made: a) All species in the stagnation gas cap are in thermodynamic equilibrium. (The distribution of energy in all internal modes of all species corresponds to the same temperature, and that temperature is the static temperature of the gas.) b) The radiant emission of the spectral lines is not appreciably self-absorbed;

i.e. the copper lines are optically thin; c) The contribution of free stream copper line emission is negligible compared to the intensity radiating from the gas cap; d) Absorption by ambient air in the optical path has a uniform and negligible effect; e) Any one spectral datum is unaffected by tunnel unsteadiness.

The assumption of thermodynamic equilibrium (a) is necessary to the experimental procedure since the copper emission lines examined are due to transitions by bound electrons of copper atoms. The temperature which results from an examination of these copper lines is the copper electronic temperature. The assumption of thermodynamic equilibrium is necessary in order to use this electronic temperature as the local static temperature.

A highly idealized analysis was made to determine the order of magnitude of the degree of nonequilibrium present in a stagnation gas cap on a blunt body under typical test conditions. For the typical re-entry test conditions chosen, the reservoir total pressure is 100atm, the free stream Mach number prior to the bow shock is 1.8, and the free stream static temperature is 4300°K. For these initial conditions, the histories of

the electronic states bound to the copper atoms must be traced through the shock wave to determine at what distance the electronic states come into equilibrium with the static temperature behind the shock. The analogous, order of magnitude, theoretical approach chosen is the examination of a calorically perfect mixture of molecular nitrogen and free electrons initially at 4300 K and Mach 1.8. The initial total pressure is chosen to be 100 atm which is the typical heater reservoir pressure. The nitrogen and free electron mixture is theoretically passed through a normal shock with γ assumed constant and equal to 1.2. Based on the work of McGregor and Brewer: it is assumed that the free electrons in the flow are in equilibrium with the bound electronic states at all times, and therefore, the history of the free electron temperature is assumed to conform to the bound electron temperature of all species (in this theoretical case, only molecular nitrogen). Referring to Figure 4, thermodynamic equilibrium is assumed in front of the shock wave. Therefore, the vibrational, rotational, bound electron, and free electron temperatures are all assumed to be equal to the initial static temperature of 4300°K. After passing through the shock front, the

the calorically perfect assumption gives a static temperature of 5500°K. It is left to determine the relaxation history of the bound electrons from 4300 to 5500°K.

With the help of Dr. S. S. Lazdinis[9], the electronic energy relaxation equation was examined and reduced under the following assumptions:

1) Calorically perfect process with $\gamma = 1.2$
2) Steady, one-dimensional flow
3) No reactions
4) Adiabatic flow
5) Radiation effects are negligible
6) No diffusion effects
7) Collisions are elastic,i.e. energy transfer is described through the use of collision loss factors
8) No charge separation, i.e. the electron ordered velocity is equal to the flow velocity.
9) Collisions between electrons and nitrogen molecules are much more frequent than collisions between electrons and other free electrons.

This results in a weakly ionized Maxwellian plasma with translation, rotation, and vibration coupled free electrons, where the free electron temperature is equal to the bound electronic temperature. The resulting energy

relaxation equation, applying the above assumptions, is[9]:

$$\frac{dT_e}{d_x} = -\frac{\delta_v}{U_e}\left(T_e - T_v\right)\nu_c - \frac{\delta_{tr}}{U_e}\left(T_e - T_s\right)\nu_c \qquad (1)$$

In the above equation, T_e is the free electron temperature at any point x where x=0 conforms to the shock front, and x is the distance through the normal shock; δ_v is the collision loss factor describing the transfer of energy in a collision interaction between a free electron and a nitrogen vibrational state; δ_{tr} is the collision loss factor combining the translational and rotational modes in a collision between a free electron and a nitrogen molecule; T_v is the nitrogen vibrational temperature at any points; U_e is the free electron ordered velocity which is assumed equal to U_2 (Fig 4) which is calculated from fundamental calorically perfect relations to be 8.22 x 10 5mm/sec; ν_c is the collision frequency between free electons and molecular nitrogen; and T_s is the static temperature behind the shock front which is assumed to remain constant at 5500°K.

If the total vibrational energy contained in the molecular species is assumed to be much greater than the translational energy associated with the free elec-

trons, the vibrational temperature may be assumed to be independant of the free electron temperature. Combining this assumption with the formerly stated assumptions, the Landau-Teller equation may be written as[10]:

$$T_v(x) = T_s - \left(T_s - T_{v_i}\right) \exp\left(-x/U_e\tau\right) \tag{2}$$

In equation (2), $T_v(x)$ is the vibrational temperature at any point x; T_{v_i} is the vibrational temperature at x=0 which is assumed to be equal to T_1; and τ is the vibrational relaxation parameter. In order to solve equation (1), the expression in equation (2) is substituted for T_v, and the parameter δ_v, δ_{tr}, U_e, and τ are held constant. Solving the resulting differential equation by the method of Integrating Factors, $T_e(x)$ may be expressed as:

$$T_e(x) = T_s + \left(T_{v_i} - T_s\right) \frac{\delta_v U_e \exp\left(-x/U_e\tau\right)}{U_e\left(\delta_v + \delta_{tr}\right) - 1/\tau}$$

$$+ \left(T_{v_i} - T_s\right)\left[1 - \frac{\delta_v U_e}{U_e\left(\delta_v + \delta_{tr}\right) - 1/\tau}\right] \exp - U_e x \left(\delta_v + \delta_{tr}\right)/U_e$$

As mentioned previously, T_s is held constant at 5500°K. At x=0, T_e and T_v are set equal to the static temperature T_1, prior to the shock front which is 4300°K. From normal shock relations, p_2-60 atm and U_2=8.22x10^{5}mm/sec which is assumed equal to U_e. The collision frequency

ν_c between electronic and molecular nitrogen is a function of both pressure and temperature, and is chosen from Sutton[11] to be constant at $3.60 \times 10^{14} sec^{-1}$ corresponding to the above values for p_2 and T_s. Similarily, τ is chosen from Vincenti and Kruger[10] and is held constant at 1.34×10^{-7} sec. The values for δ_v and δ_{tr} are also functions of temperature. For this analysis, they are assumed to be constant, and are chosen for characteristic values between 4300 K and 5500 K. The value of δ_v is 7×10^{-4}, and the value for δ_{tr} is found by combining $\delta_t + \delta_r$ resulting in 4.3×10^{-4}. These last two values were supplied by Lazdinis[9] who referenced the work of Demetriades[12].

When the above parametric values are substituted into equation (3), the resulting expression is:

$$T_e(x) = 5500 - 746.5e^{-9.09x} - 453.5e^{-(4.93 \times 10^5)x} \qquad (4)$$

Two plots of T_e v.s. x are shown in Figure 5. Plot "a" shows that the electronic temperature comes reasonably close to equilibrium in 0.2 mm. The sharp increase seen in plot "a" is expanded in plot "b". The sharp initial increase is the effect of term (c) in equation

(4), which is basically the translational and rotational interaction term. The slope becomes less steep as the effect of vibrational coupling (term b in equation 4) becomes dominant.

It must be reiterated that the above analysis can only be expected to have order of magnitude accuracy when it is considered analogous to the relaxation of bound copper electrons in the stagnation gas cap. Experimental evidence of thermodynamic equilibrium will be presented in a later portion of the paper.

The assumption of optical thinness has been verified experimentally (as will be explained later) for the copper lines at 5106, 5154, and 5218 Å. It is interesting to note that the copper number density and temperature generally present in the stagnation gas-caps are (fortuitously) very similar to the number density and temperature at which the NBS thermodynamic data for copper was generated[13]. Corliss and Bozmann[13], who did the NBS experiment, state their copper number density as approximately 10^{17}/cc at a temperature of 5000°K. In a stagnation gas cap at 60 atm and 5500°K, the perfect gas law predicts a total number density of 10^{20}/cc. From electrode erosion measurements, the copper number

density in stagnation gas caps is expected to be 0.1% or less of the total number density. This would place the stagnation gas cap copper number dnsity at 10^{17}/cc or less.

In their NBS Monograph, Corliss and Bozmann[13] make no mention of correction for self-absorption effects in the copper lines. Therefore, the NBS data appears to have been generated under an optically thin assumption in a plasma at 5100°K with a copper number density of 10^{17}/cc. The fortuitous comparison between the NBS copper number density led the authors to assume, initially, that the gas caps were optically thin with respect to all copper lines. For some lines, however, this assumption was erroneous, as will be explained later.

Non-interference of free stream copper line emission is justified experimentally , since the magnitude of the absolute intensities of free stream copper lines is found to be approximately 1/100 of the copper line radiating from a stagnation gas cap. The background continuum is readily subtracted from spectral data for enthalpies above 2000 BTU/lb, but below this value, the copper line intensities are so low that they cannot

readily be distinguished from unsteadiness displayed in the continuum. This delineates the lower limit of the technique; however, the high heating rate tests for which the spectral measurement of enthalpy is employed, are generally at enthalpies well above 2000 BTU/lb.

The absorption effects by ambient air were expected to be negligible, and this was found to be true by examination of a mercury spectrum over distances from one to 15 ft from the entrance optics of the spectograph. The reduction of heater unsteadiness effects has been previously discussed.

Once the spectral data has been taken, the copper lines are analyzed by ratioing any two of them in a standard technique based on the following well-known theory[14]. The intensity of any optically thin electronic transition line is expressed as:

$$I_n^m = h\nu_o N \frac{A_n^m g_m}{Z_o} e^{-\frac{E_m}{kT_e}} \qquad (5)$$

where m denotes the upper electronic state and n is the lower state. $A_n^m g_m$ is the transition probability for the particular line examined, Z_o is the partition

function for the species producing the spectral line, h is Planck's Constant, ν_o is the spectral line frequency, E_m is the upper state energy, k is Boltzmann's constant, and T_e is the electronic temperature of the species emitting the spectral line.

The ratio of two lines of the same species is then expressed as;

$$\frac{I_n^m}{I_{n'}^{m'}} = \frac{A_n^m g_m \nu_o}{A_{n'}^{m'} g_{m'} \nu_{o'}} e^{-\frac{(E_m - E_{m'})}{kT_e}} \tag{6}$$

Solving for T_e results in:

$$T_e = \frac{E_{m'} - E_m}{k \ln \left(\frac{I_n^m A_{n'}^{m'} g_{m'} \nu_{o'}}{I_{n'}^{m'} A_n^m g_m \nu_o} \right)} \tag{7}$$

The values for E_m and $A_n^m g_m$ can be found in reference 13, and each I_n^m is a measured value. Therefore, from two well defined copper lines, T_e can be determined. When the stagnation region is the region analyzed, T_o, the total temperature, is equal to T_e under the assumption presented earlier.

Once an experimental total temperature has been determined, H_o may be calculated from T_o and a measured value of P_{o_2} with standard equilibrium air calculations. These calculations form the well known Mollier diagram

which has been simplified by Doyle and Boison[15] for the range of interest in this paper. The approximation derived is:

$$H_o = 1.143\,T(^\circ K) - 223 \ln P_{O_2}(atm) - 1112 \text{ BTU/lbm} \tag{8}$$

This relationship holds within $\pm$ 2% for air at $4300 \leq T_o \leq 6000$ K, and $5 \leq P_{O2} \leq 100$ atm.

Experimental Results and Conclusions

Spectral data has been taken and analysed in both the AFFDL 4 MW Hypersonic facility and in the 50 MW re-entry facility. Copper lines have been recorded at 3248, 3274, 5106, 5153, 5218, 5220, 5700, and 5782 Å. The energy levels and term combinations for these lines are given in Table 1.

Preliminary data was taken in the 4 MW hypersonic facility to determine whether or not ablation species would hinder spectral analysis of the gas cap. Complete spectra were taken from 2500 to 6500 Å on two blunt models of different materials. For the same reservoir conditions, the spectrum from the stagnation gas cap on a wood blockage model was identical to the spectrum from the stagnation gas cap on 1 inch nose radius copper calorimeter. The only situation in

which ablation species interfere with the spectral data is when the optics are mis-focussed, and the model surface is in the field of view.

The preliminary data in the 4 MW facility shows the dominant spectral properties to be the copper lines at 3248 and 3274 Å. The 5220 Å line is combined with the 5218 A line, since the spectrometer employed has 4 Å resolution. The 5220 Å line provides about 15% of the radiation at that position. The lines at 5700 and 5782 Å appear only weakly in the 4 MW facility data.

In the 50 MW RENT facility, where the preponderance of the spectral measurement work has been done, the above copper lines are again found to dominate the spectrum. It is in the RENT facility where these lines were first resolved and analysed for a total enthalpy measurement.

In figure 6a is shown a spectrum of the 3248 and 3274 Å copper lines from a stagnation gas cap at approximately 5500°K and 60 atm. This spectrum is strong evidence that not all the copper lines seen emitting from a stagnation gas cap can be considered optically thin. This particular pair exhibits strong line broadening, seen in the "wings", and self-absorbed

line centers showing characteristics of optical thickness. Since the optical thinness assumption cannot apply to these two lines, they have been discarded as candidates for the measurement of stagnation, or total temperature.

Figure 6b shows typical data for the 5106, 5153, and 5218-5220 Å copper lines. These lines have been examined for stagnation gas cap conditions ranging from 4.5 to 80 atm, and from 3000 to 6500°K. In none of these cases did these lines exhibit the properties of the lines in Figure 6a.

A good check on both the thermodynamic equilibrium and optical thinness assumptions has been accomplished by keeping the heater, reservoir, and throat conditions constant for two different nozzle exit areas. In both cases, the heater-reservoir was at 100 atm and approximately 5500°K. The nozzle throats in each case were .9 inches in diameter. In one case, the exit diameter was 1.1 inch, while in the second case, the exit diameter exceeded 4 inches. In both cases, the models to be tested were placed 0.1 inch downstream of the nozzle exit plane. In case 1 the stagnation pressure on the model (P_{o2}) was measured to be 80 atm, while in case 2, the measured model stagnation pressure was only 5 atm;

a factor of 16 lower. For these two cases, the total enthalpy in the stagnation region should have been the same (same reservoir conditions), but the heating rate in case 2 should have been much lower due to the much lower pressure in the model gas cap. The data for the two cases is presented in Tables 2 and 3.

For both cases, the 5106, 5153, and 5218-5220 Å spectra appeared very nearly identical, gave similar temperatures from the line ratios, and resulted in spectrally measured enthalpies differing by approximately 5%. Since both cases were run for a "peaked" enthalpy condition (Fig 1), it is not surprising that the more expanded case gave a 5% lower enthalpy, since the enthalpy "peak" had more time and distance to disperse. The significant result is that by holding temperature virtually constant, but varying pressure (i.e. number density through the perfect gas law) by a factor of 16, the spectral data from the ratios of the 5106, 5153, and 5218-5220 Å lines remained nearly identical, as they should for nearly identical temperatures. Therefore, self-absorption effects are either negligible or uniform for the three lines such that the optical thinness assumption holds in this range. Also, since the degree of non-equilibrium is pressure dependent

for identical temperatures and species at a point in an expansion or compression process, it can be assumed that thermodynamic equilibrium existed in the stagnation region for both cases, since the data was consistant.

A typical spectrum of the 5700 to 5782 Å copper lines is shown in Figure 6c. These two lines are approximately a factor of 5 less intense than the lines around 5100-5200 Å, and they occur in a region where a combination of phototube response and strong continuum produce a slanting spectral baseline, which makes data reduction difficult. There is also enough spectral "noise" in this region to interfere with the copper lines, increasing the possibility of error. The result is that the copper lines at 5106, 5153, and 5218-5220 Å are the lines which are now being used for total enthalpy measurement.

The general method of data accumulation and analysis is as follows. Prior to the test, the rapid-scanning spectrometer is focussed just upstream of a model placed in test position. When the test is under way, the RENT automatic axial drive system will keep the physical position of the model blunt nose constant, with respect to the nozzle exit, as the nose ablates.

Once the focussing is accomplished, the oscilloscope, on which the data is read, is turned on, and a 40 frame/second framing camera is placed to record the data on 100 feet of 35 mm film. When the facility is started, the oscilloscope is adjusted so that the amplitudes of copper lines from free stream emission are just barely visible. The scope is then expanded so that only the spectral region from 5000 to 5400 Å is displayed. As the model enters the test section, the copper line intensity from the stagnation region is approximately 100 times that of the free stream, so that the stagnation gas cap emission lines are fully displayed on the scope. The framing camera records the data and the resulting film is processed into rolls of 8 x 10 prints. From each of these prints, data such as Figure 6b is analysed for the line ratios 5106/5153 and 5106/(5218+5220) Å using equation (7).

It has been found that assuming the 5106/5218+5220) Å is actually 5106/5218 produces a temperature and enthalpy error of + 5% at 5000°K and + 4% at 7000°K. Since this is the range most often examined, it is felt that considering the 5106/(5218+5220) line ratio to be actually 5106/5218, and correcting the resultant temperature by -4.5%, produces an acceptable error of

$\pm$ 0.5%. The analysis is simplified considerably in this manner.

The ratio of 5153/5218 is not used, since the closeness of the energy levels of the upper electronic states produces a small difference of large numbers in equation 7, and the effect of errors becomes large in that equation.

The parameters chosen for equation (7)[13], and the method of data reduction are combined in Figure 7 which was generated by Boison and Doyle[15]. From this graph, one is readily able to evaluate enthalpy from each copper line spectrum. On an average run, between 20 and 40 spectra are taken while a model is pinned on the test section centerline. The total time involved is less than a second, and each spectrum contains the three lines from which the two line ratios are formed. Total temperature is determined for each line ratio for each spectrum, giving up to 80 values fo a 1 second test. The 80 values are statistically analysed to give a mean total temperature. This temperature is then combined with the measured P_{O_2}, and compared with a Mollier diagram to give a mean total enthalpy for the model test. Figure 8 shows a 1/2" radius, flat nose, blunt model under test in the AFFDL 50 MW Re-entry Test

Leg, and Table 3 lists the resulting data from that model during 1.5 seconds of test time. A histogram of the 80 data points presented in Table 3 is given in Fig 9.

At heating rates below 5000 BTU/ft^{2}sec, steady state calorimeters and enthalpy probes have been used successfully to integrate unsteadiness effects and produce a meaningful value of total enthalpy. Generally, these lower heating rates are produced at total enthalpies below 2500 BTU/lbm; a region in which the spectral measurement procedure has not proven fruitful. At these less extreme conditions, the steady state calorimeters are better than the spectroscopic methods for two reasons: a) The calorimeters read the actual heating effects due not only to total enthalpy and pressure, but also due to any high frequency low amplitude flow unsteadiness; and, b) The signal to noise ratio of the copper lines becomes disadvantageous at values of total enthalpy below 3000 BTU/lbm.

Much of the spectral data shows evidence of a high frequency oscillation (300Khz) of low amplitude present in the flow field. There is some speculation[16] that this high frequency unsteadiness could cause heat transfer on a model which would be greater than characteristic of the total enthalpy present in the test section. The small amount of calorimeter data avail-

able is scattered for high enthalpy test conditions, but it does generally fall above the spectroscopic data. The high frequency oscillation is cited as a possible reason for this discrepancy.

In Table 4 is presented some of the scattered transient calorimeter data for tests conforming to the reservoir conditions of the data presented in Table 2. The range of data in Table 4 compare favorably to the range of data in Table 2, which is further encouraging for the spectral measurement technique; however, the data also points out the difficulty of using transient enthalpy probes at high heating rate-high enthalpy conditions when heater unsteadiness is present. As previously stated, the dominant oscillation frequency in the arc heater is near 100hz. The "peaked" portion of the flow field (Fig. 1) is the portion used for test, and the transient probes pass through this portion of the flow in less than 10 msec, which is less than the characteristic period of oscillation of the heater. From Table 3, the unsteadiness amplitude can be seen to cover a range of $\pm$ 15% of the mean. Therefore, any transient probe point could easily be in error by as much as 15% assuming all theories connected with transient probe data reduction are

absolutely correct. This means that any transient probe measurement of peaked enthalpy must take the heater unsteadiness into account either by taking a statistically meaningful sample of points, or by moving the probe slowly enough so that the unsteadiness effects are integrated out. The latter is hard to accomplish when the heater is operating under extreme heating conditions above 5000 BTU/ft^2-sec.

In conclusion, it can be generally stated that the spectroscopic measurement of total enthalpy is now considered valuable as a complement to calorimetry for total enthalpy measurement in the AFFDL Re-entry facility. Above enthalpy levels of 3000 BTU/lbm, the spectroscopic method is able to measure total enthalpy in the stagnation gas cap on a model as the model is undergoing a test. The spectroscopic method delineates the unsteadiness effects, giving the range and the mean for the peaked enthalpy conditions. Below 3000 BTU/lbm, and 5000 BTU/ft^2-sec, probe methods can be used in such a manner that the heater unsteadiness is integrated over a period of time, and a good measurement results. Also, below 3000 BTU/lbm, the spectroscopic method has had little success.

Employing calorimetric and spectroscopic methods in

their respective regions of application, measurements of total enthalpy may now be made throughout the test regime of the AFFDL 50 MW Reentry facility.

References

1. J. L. Folck and R. T. Smith; "Hypersonic Flow Diagnostic Studies in a Large Arc-Heated Wind Tunnel", AIAA Journal. Vol. 8, and related unpublished work.

2. L. R. Lawrence, Jr. and James T. Van Kuren; "Total Enthalpy Measurement From Blunt-Body Gas Cap Emission in Hypersonic Wind Tunnels; Part I", International Congress on Instrumentation in Aerospace Simulation Facilities, Brussels, Belgium, June 1971.

3. W. S. Kennedy, R. A. Rindal, C. A. Powers; "Heat Flux Measurement Using Swept Null Point Calorimetry," AIAA Paper, No. 71-428.

4. J. A. Fay and F. R. Riddell; "Theory of Stagnation Point Heat Transfer in Disassociated Air," Journal of the Aerospace Sciences, Vol. 25, No. 2, February 1958.

5. T. M. Weeks; "Effects of Flow Unsteadiness on Hypersonic Wind-Tunnel Spectroscopic Diagnostics," AIAA Journal, Vol. 8, No. 8.

6. J. T. Van Kuren; "Experimental and Theoretical Investigation of the Nozzle Flow in a Large Arc-Heated Hypersonic Wind Tunnel", PhD Dissertation, Ohio State University, (1969).

7. R. F. Weber and A. Garscadden; "Errors Due to Averaging Spectral Line Intensities in the Presence of Electron Temperature Variations", J. Opt Soc. Am. Vol. 61 No. 10.

8. W. K. McGregor and L. E. Brewer; "Equivalence of Electron and Excitation Temperatures in an Argon Plasma" Physics of Fluids, Vol. 9, 1966.

9. S. S. Ladinis; Private Communication.

10. Walter G. Vincenti and Charles H. Kruger, Jr.; Introduction to Physical Gas Dynamics, John Wiley and Sons, Inc., New York 1965.

11. G. W. Sutton and A. Sherman; Engineering Magnetohydrodynamics, McGraw-Hill book Co., New York 1965.

12. S. T. Demetriades; Determination of Electron Energy-Loss Factors in Hot Gases", STD Research Corporation Report. STD-68-2 (August 1968).

13. Charles H. Corliss and William R. Bozman: Experimental Transition Probabilities for Spectral Lines of Seventy Elements, NBS Monograph 53.

14. Gerhard Herzberg; Atomic Spectra and Atomic Structure; Dover Publication, New York(1944) 2nd edition.

15. Joseph P. Doyle, Jr. and J. Christopher Boison, "Conversion of Spectrographic Measurements to Total Temperature and Enthalpy in the AFFDL 50 Megawatt Rent Facility"; AFFDL/FX-TM-72-13 Air Force Flight Dynamics Laboratory, March 1972.

16. E. G. Brown-Edwards, Private Communication, Air Force Flight Dynamics Laboratory, Wright-Patterson AFB, Ohio (1972)

17. William F. Meggers, Charles H. Corliss, and Bourdon F. Scribner; Tables of Spectral Line Intensities; NBS Monograph 32, Part I, December 29, 1961.

TABLE 1

Copper line energy levels and Term Values[17]

Wavelength (Å)	Energy Levels(K)	Term Combination
3247.54	0-30784	$3d^{10}\ 4s\ ^1S_{0\frac{1}{2}}$-$3d^{10}\ 4p\ ^2P_{1\frac{1}{2}}$
3273.96	0-30535	$3d^{10}\ 4s\ ^1S_{0\frac{1}{2}}$-$3d^{10}\ 4p\ ^2P_{0\frac{1}{2}}$
5105.54	11203-30784	$3d^9\ 4s^2\ ^2D_{2\frac{1}{2}}$-$3d^{10}\ 4p\ ^2P_{1\frac{1}{2}}$
5153.24	30535-49935	$3d^{10}\ 4p\ ^2P_{0\frac{1}{2}}$-$3d^{10}\ 4d\ ^2D_{2\frac{1}{2}}$
5218.20	30784.49942	$3d^{10}\ 4p\ ^2P_{1\frac{1}{2}}$-$3d^{10}\ 4d\ ^2D_{2\frac{1}{2}}$
5220.07	30784-49942	$3d^{10}\ 4p\ ^2P_{1\frac{1}{2}}$-$3d^{10}\ 4p\ ^2P_{1\frac{1}{2}}$
5700.24	13245-30784	$3d^9\ 4s^2\ ^2D_{1\frac{1}{2}}$-$3d^{10}\ 4p\ ^2P_{1\frac{1}{2}}$
5782.13	13245-30535	$3d^9\ 4s^2\ ^2D_{1\frac{1}{2}}$-$3d^{10}\ 4p\ ^2P_{0\frac{1}{2}}$

TABLE 2

Data from a 0.25 inch radius graphite hemisphere-cone taken during a time interval of 0.7 seconds.

λ_1 A	λ_2 A	I (relative intensity)	I_1/I_2	T °K
	5106	25.5		
5153		18.8	0.737	5718
5218		26.8	1.05	5646
	5106	16.7		
5153		10.7	0.641	5556
5218		16.4	0.982	5565
	5106	27.0		
5153		12.9	0.477	5246
5218		16.8	0.62	5075
	5106	35.0		
5153		24.2	0.691	5643
5218		3314	0.954	5531
	5106	16.4		
5153		6.8	0.415	5108
5218		9.2	0.561	4976
	5106	14.8		
5153		8.8	0.595	5474
5218		12.5	0.845	5393

P_{t_2} =80 atm.
Mean=5411°K
Standard deviation=250.0
Probable error=168.7°K
Mean enthalpy=4096 BTU/lbm

TABLE 3

Calibration Test RTN-33-029 25 April 1972

P_{t_2}=5.5 ATM

I_{5153}	←→T←→	I_{5106}	←→ T←→	I_{5218}
0.205	4381°K	1.21	4237°K	0.27
0.135	4345°K	0.84	4210°K	0.18
0.75	5196°K	1.65	5410°K	1.415
0.18	4670°K	0.72	4594°K	0.26
0.905	5400°K	1.63	5224°K	1.065
0.585	4975°K	1.63	4930°K	0.87
0.13	4352°K	0.80	4511°K	0.26
0.30	4637°K	1.25	4460°K	0.38
0.205	4731°K	0.76	4984°K	0.43
0.28	4909°K	0.84	4913°K	0.44
0.24	4415°K	1.35	4766°K	0.66
0.325	4676°K	1.29	4699°K	0.53
0.16	4260°K	1.13	4204°K	0.24
0.25	4449°K	1.34	4038°K	0.22
0.18	4472°K	0.935	4335°K	0.24
0.43	4930°K	1.26	4870°K	0.63
0.25	4449°K	1.34	4714°K	0.56
0.40	4834°K	1.31	4597°K	0.475
0.58	5111°K	1.395	5087°K	0.88
0.27	4594°K	1.19	4487°K	0.375
0.275	4577°K	1.24	4072°K	0.215
0.34	4738°K	1.25	4781°K	0.565
0.435	4698°K	1.68	4979°K	0.945
0.30	4683°K	1.18	4504°K	0.38
0.185	4276°K	1.275	4319°K	0.32
0.37	4585°K	1.65	4295°K	0.37
0.27	4700°K	1.04	4515°K	0.27
0.23	4617°K	0.985	4700°K	0.23
0.18	4373°K	1.075	4280°K	0.18
0.35	4681°K	1.38	3947°K	0.35
0.16	4456°K	0.85	4389°K	0.16
0.53	4932°K	1.55	4755°K	0.53
0.44	4772°K	1.55	4175°K	0.44
0.355	4582°K	1.59	4478°K	0.355
0.40	4834°K	1.31	5057°K	0.40
0.41	4858°K	1.305	4736°K	0.41

TABLE 3 (continued)

I_{5153} ←	T →	I_{5106} ←	T →	I_{5218}
0.24	4425°K	1.33	4311°K	0.24
0.485	4844°K	1.57	4692°K	0.485
0.61	5036°K	1.59	4643°K	0.61
0.385	5106°K	0.93	4479°K	0.385

mean temperature	4637°K
standard deviation	306
probable error	206.5
probable error of mean	23.1
number of data points	80
standard deviation of mean	34.2
mean enthalpy	3808 BTU/lbm

Statistical treatment assumes errors are non-systematic (random).

Enthalpy was calculated using Equation 8.

TABLE 4

Enthalpy Derived from Heat Transfer Rates Using Fay and Riddell[4] Theory.

Conical nozzle with throat diameter of 0.9" and exit diameter of 4.5".

Two models per test run using 1/4" nose radius calorimeters.

Results only given for nozzle centerline data.

TEST RUN	STRUT NO.	MAXIMUM Ho BTU/lb	MINIMUM Ho BTU/lb
024	2	4960	2910
024	3	4960	3070
025	2	5020	2680
025	3	5460	3280
026	2	4960	2830
026	3	5280	3330
027	2	5360	3700
027	3	6300	3620
028	2	5280	3300
028	3	5900	3780
029	2	5280	3300
029	3	6300	3930

Average of maxima near centerline is 5420 BTU/lb

Average of minima near centerline is 3320 BTU/lb

List of Figures

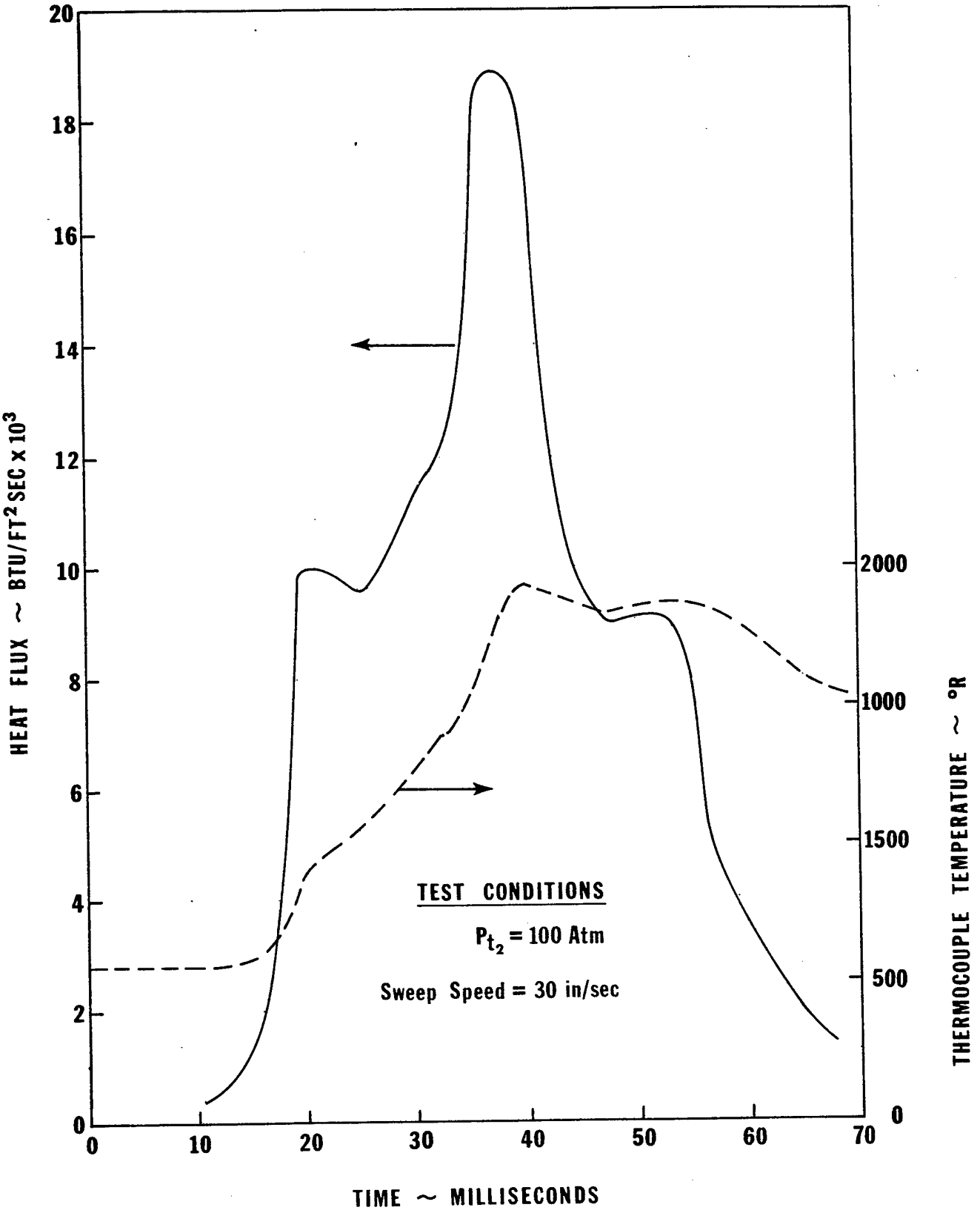

Figure 1. Peaked Enthalpy Condition As Determined By Swept Calorimeter (ref. 3)

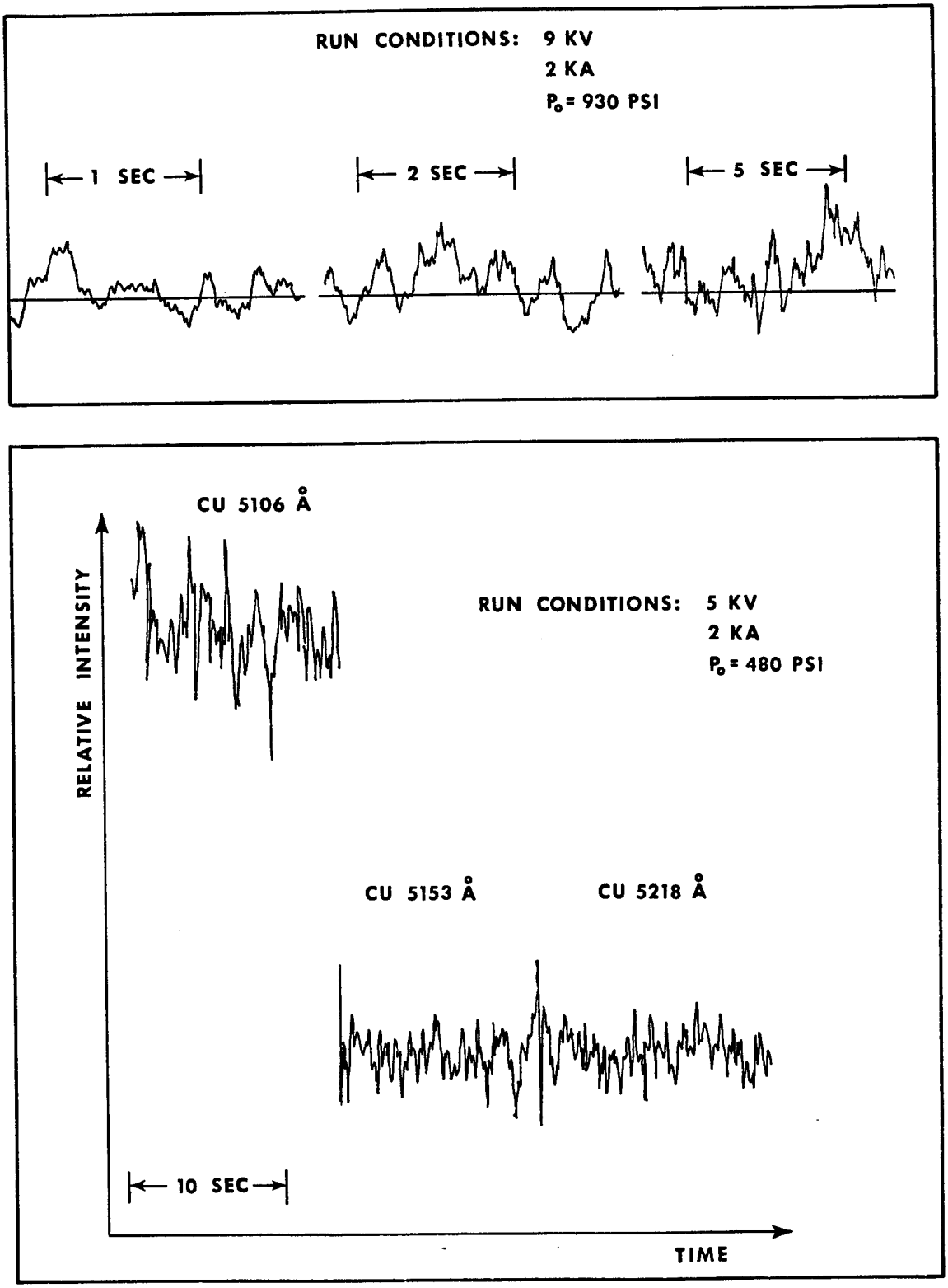

FIGURE 2. INTENSITY FLUCTUATIONS IN THE 50 MW FACILITY

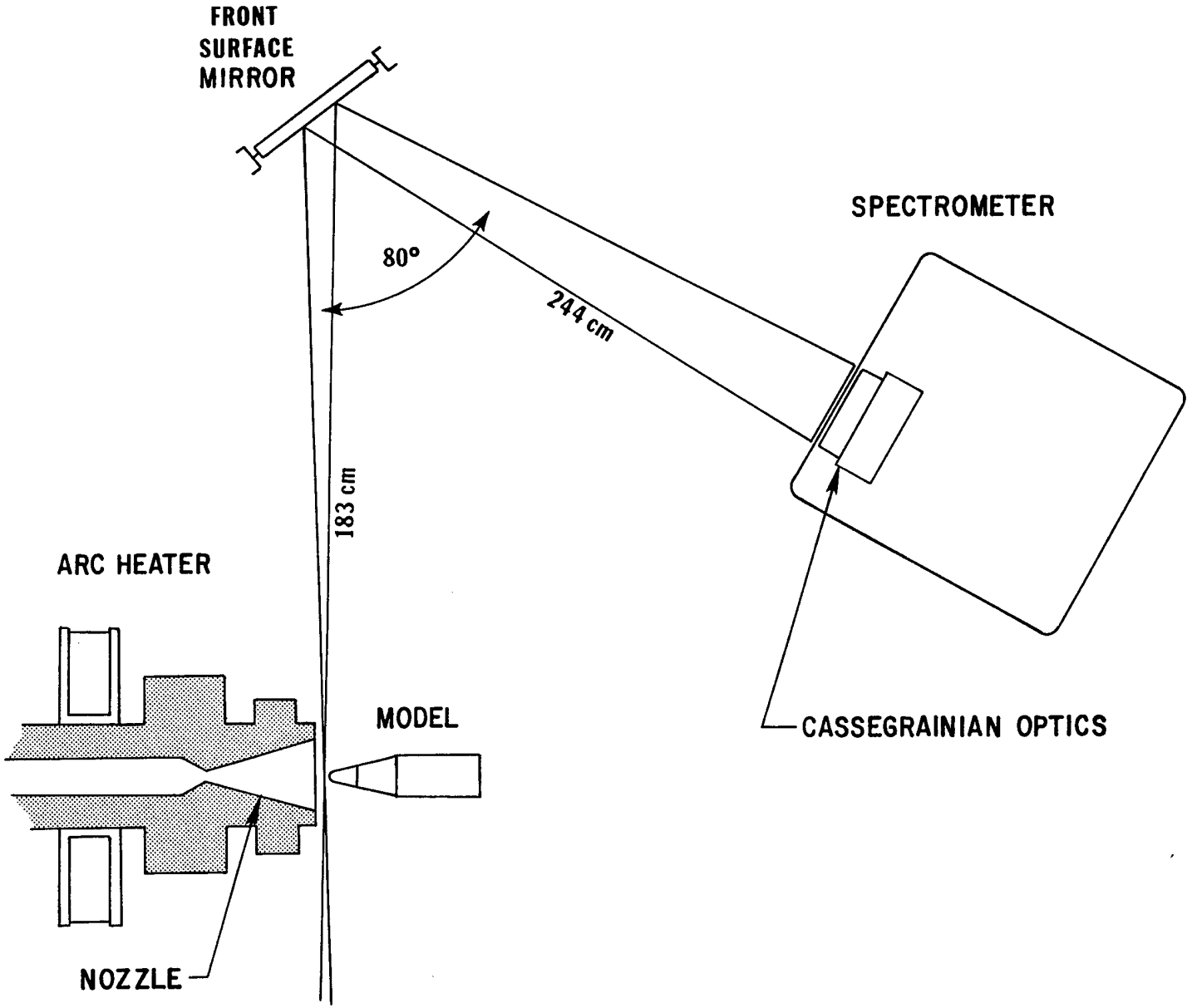

FIGURE 3. SPECTRAL DIAGNOSTICS INSTRUMENTATION

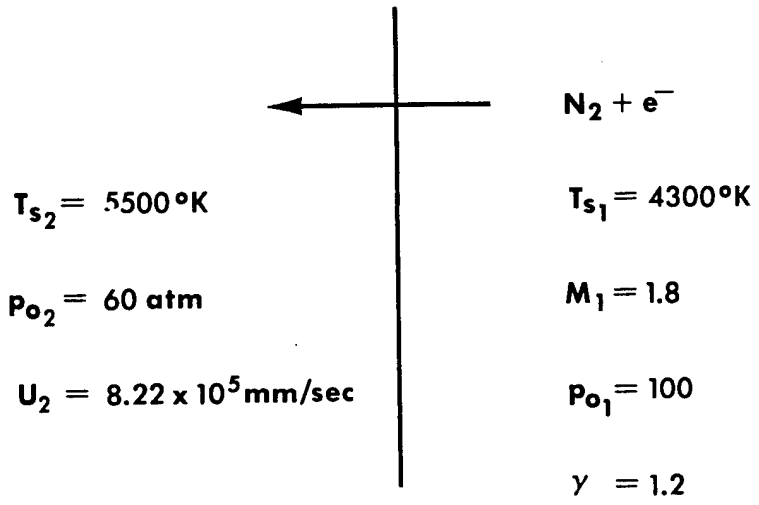

FIGURE 4. ASSUMED THEORETICAL MODEL FOR BOUND ELECTRON TEMPERATURE HISTORY; A NORMAL SHOCK WITH FLOW DIRECTION FROM RIGHT TO LEFT

$$T_e = 5500 - 7.456 \times 10^2 e^{-9.09X} - 453.5 e^{-4.93 \times 10^5 X}$$

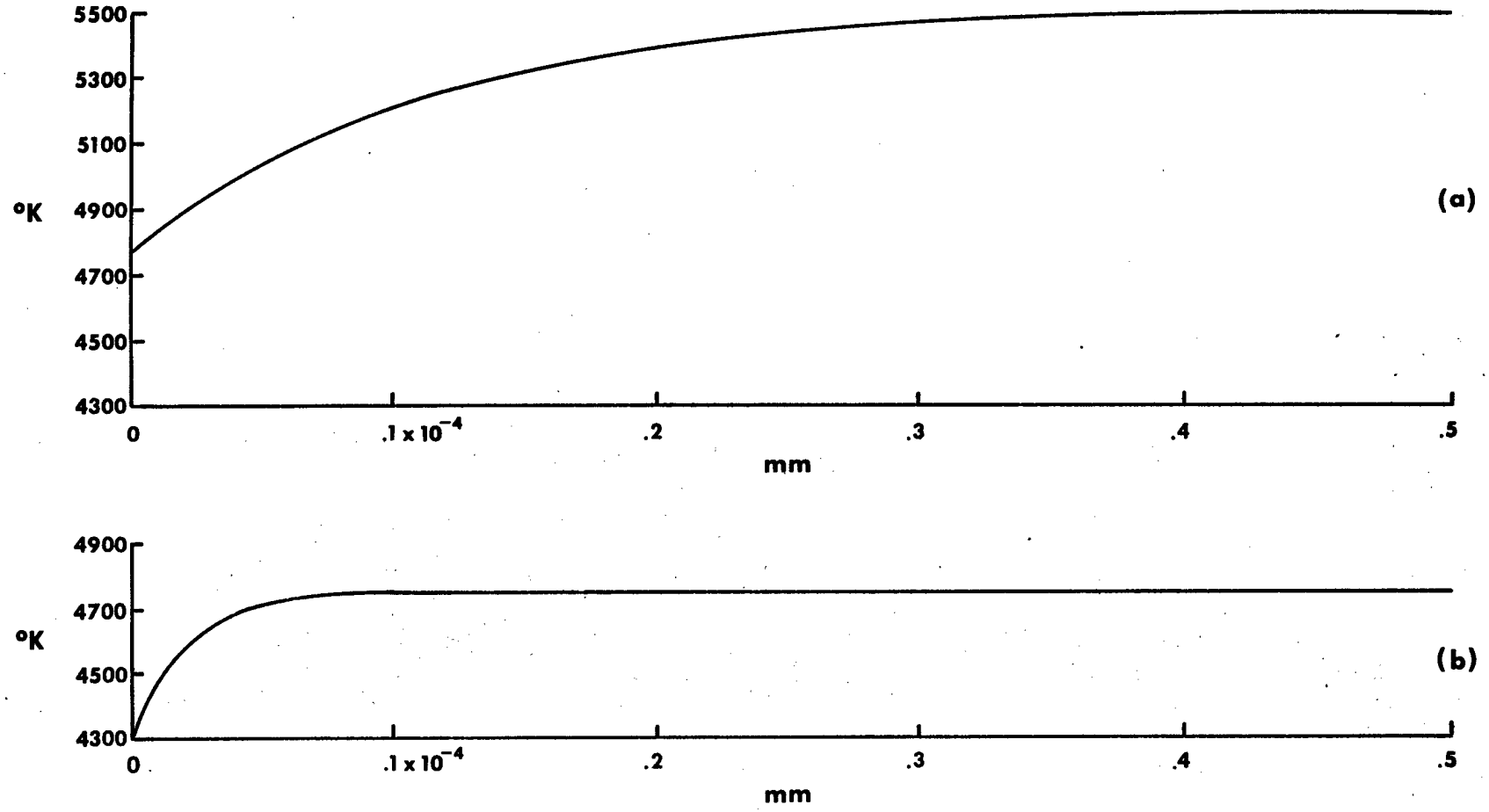

FIGURE 5. RELAXATION OF THE ELECTRONIC TEMPERATURE IN THE GAS CAP

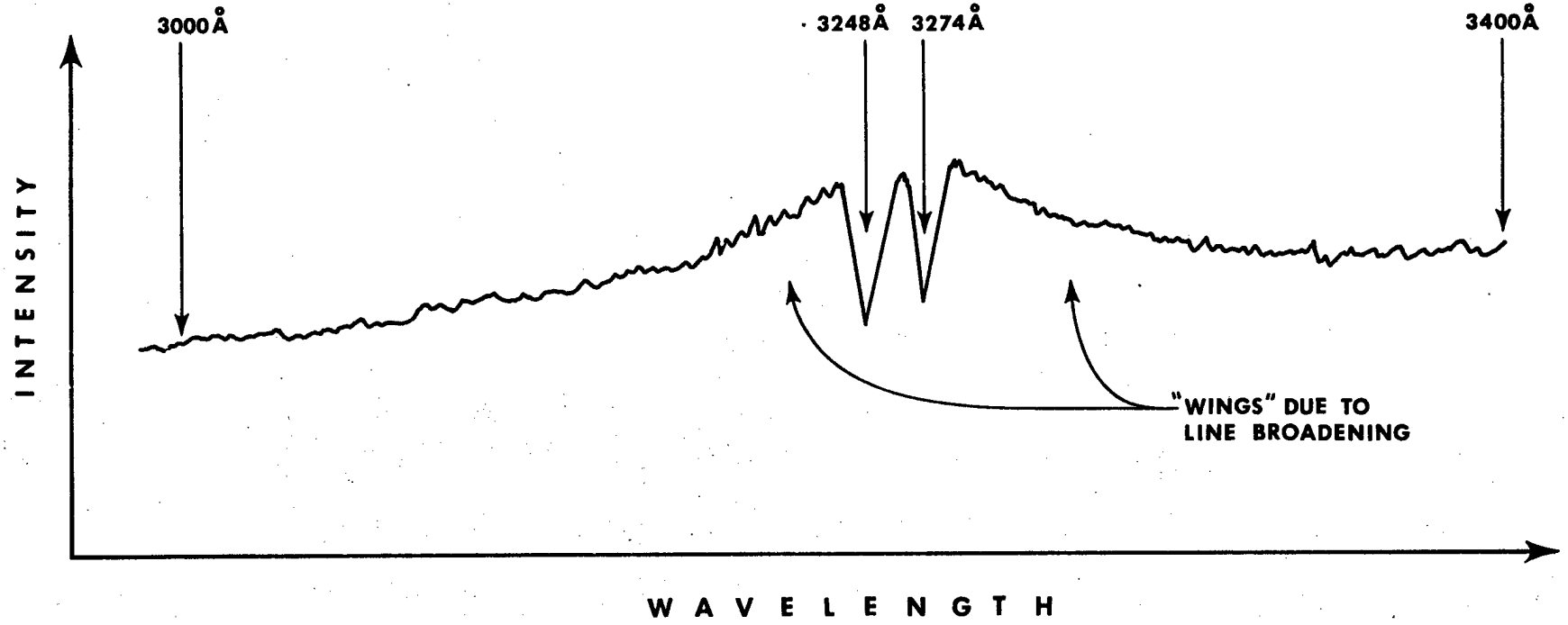

FIGURE 6a. TYPICAL DATA OF THE 3248A AND 3274A COPPER LINES SHOWING THE STRONG SELF ABSORBTION AND LINE BROADENING TENDENCIES

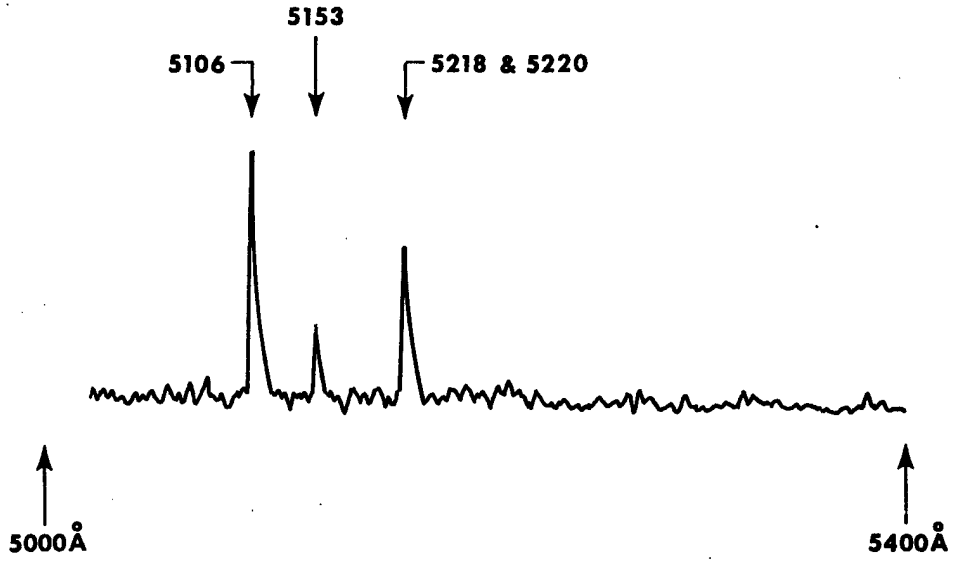

FIGURE 6b. TYPICAL OSCILLOSCOPE TRACE OF THE COPPER LINE SPECTRUM FROM 5000Å TO 5400Å

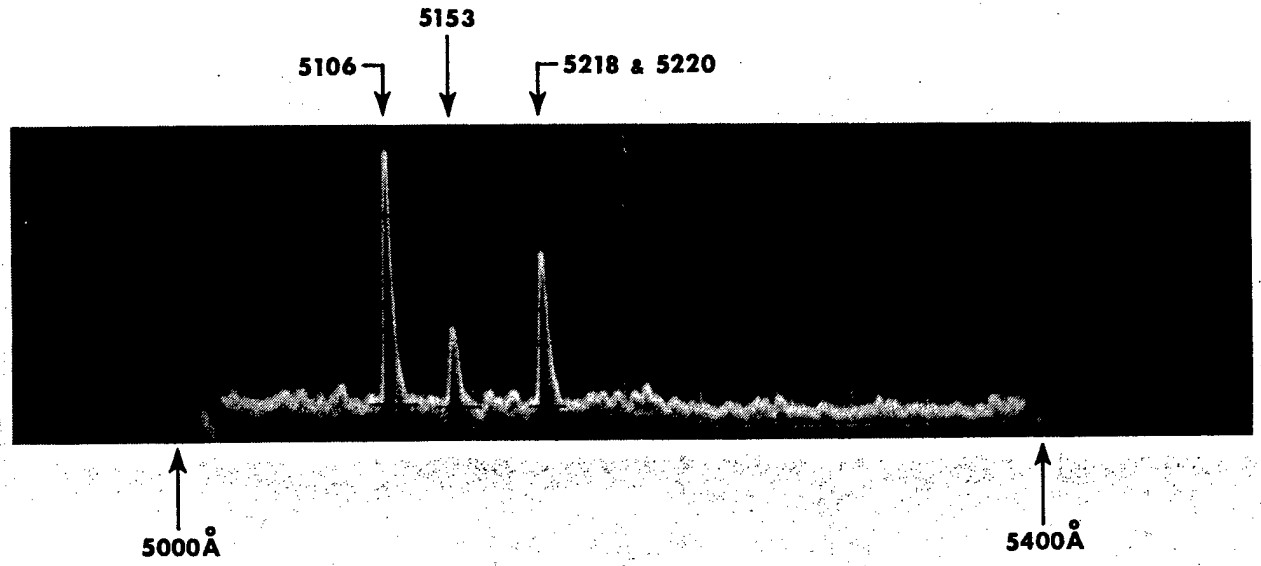

FIGURE 6b. TYPICAL OSCILLOSCOPE TRACE OF THE COPPER LINE SPECTRUM FROM 5000Å TO 5400Å

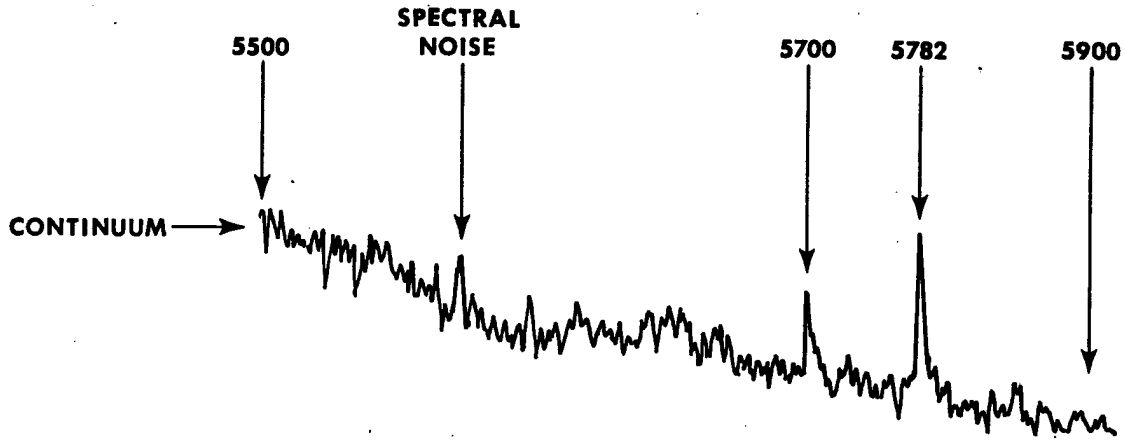

FIGURE 6c. TYPICAL COPPER LINE SPECTRUM BETWEEN 5500Å & 5900Å

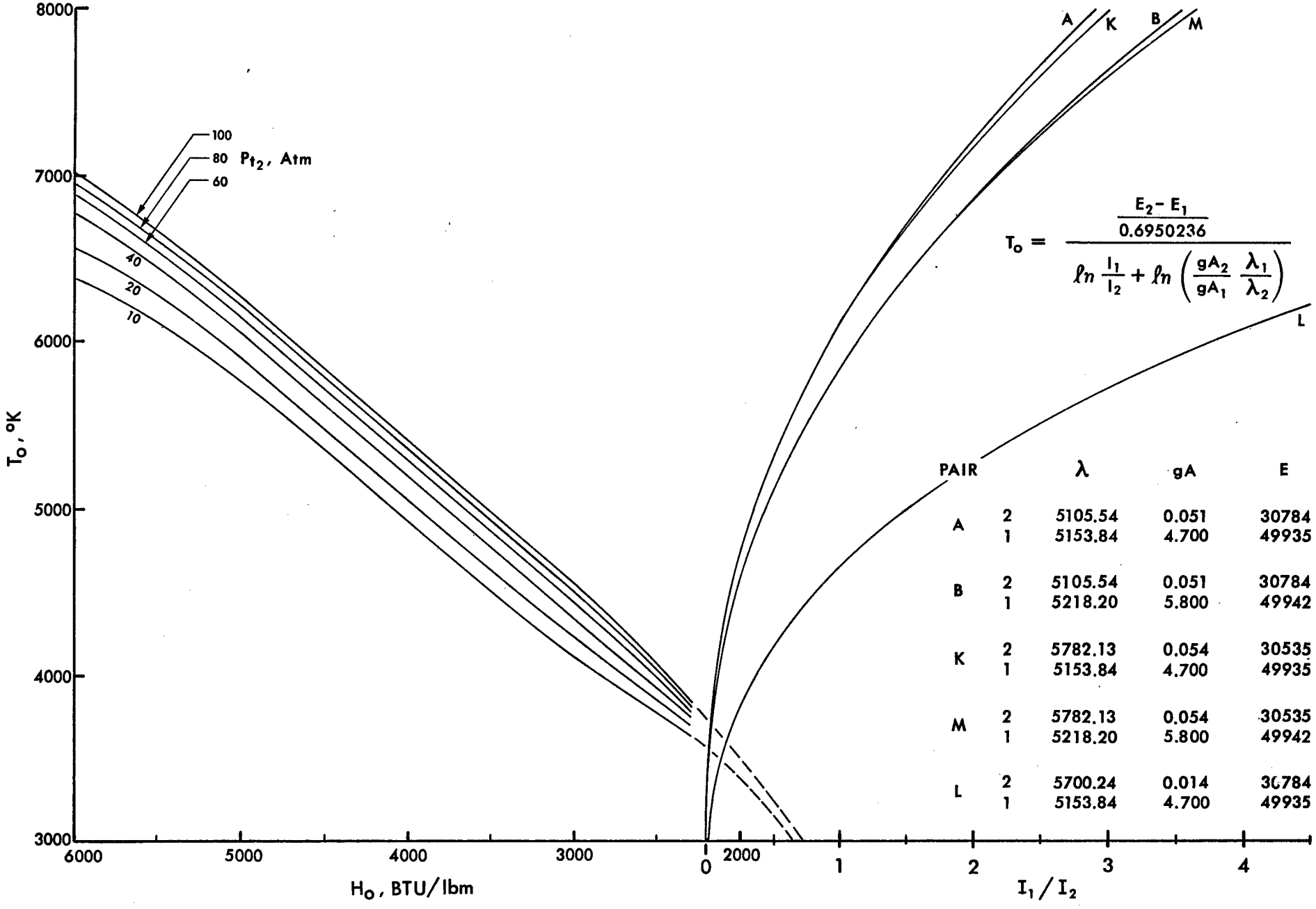

Figure 7. Calculation of Enthalpy From Intensity Ratios

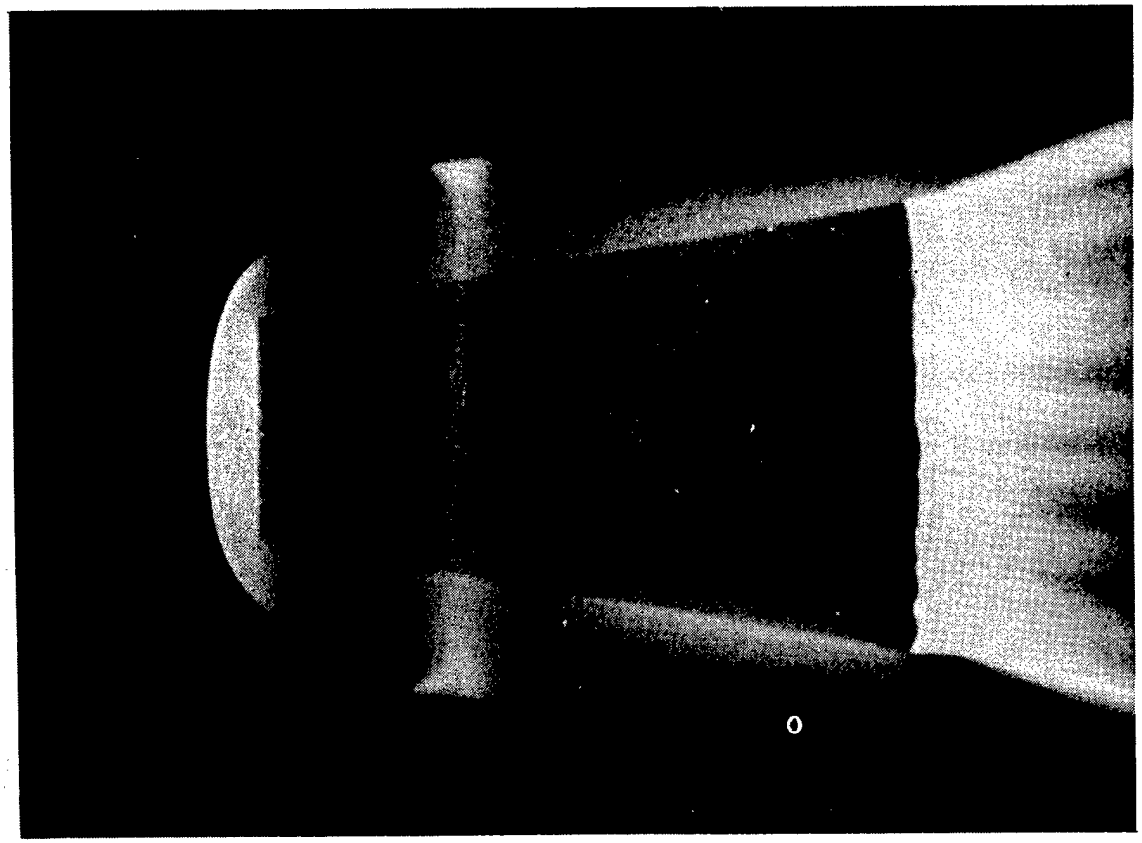

FIGURE 8. 0.5 INCH NOSE RADIUS, BLUNT GRAPHITE MODEL UNDER TEST IN THE 50MW RE-ENTRY FACILITY

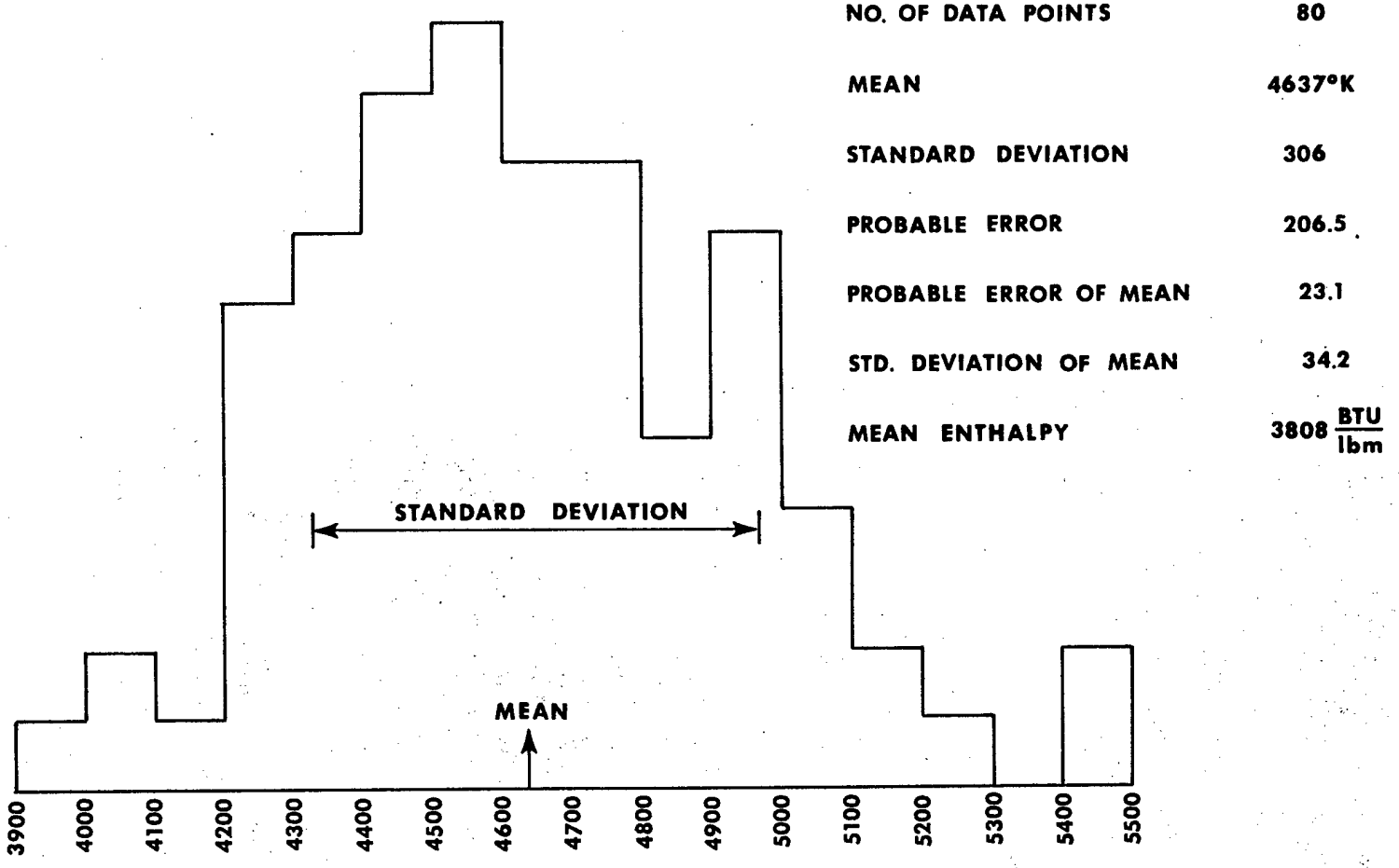

FIGURE 9. HISTOGRAM OF DATA IN TABLE 3